Green Chemistry

Green Closed-Loop Process for Selective Recycling of Lithium from Spent Lithium-ion Batteries

Journal:	*Green Chemistry*
Manuscript ID	GC-ART-05-2022-001811.R2
Article Type:	Paper
Date Submitted by the Author:	26-Jul-2022
Complete List of Authors:	Hou, Jiahui; Worcester Polytechnic Institute Ma, Xiaotu; Worcester Polytechnic Institute, Fu, Jinzhao; Worcester Polytechnic Institute Vanaphuti, Panawan; Worcester Polytechnic Institute, Mechanical Engineering Yao, Zeyi; Worcester Polytechnic Institute Liu, Yangtao; Worcester Polytechnic Institute Yang, Zhenzhen; Argonne National Laboratory, Chemical Science and Engineering Wang, Yan; Worcester Polytechnic Institute,

Green Closed-Loop Process for Selective Recycling of Lithium from Spent Lithium-ion Batteries

Received 00th January 20xx,
Accepted 00th January 20xx

DOI: 10.1039/x0xx00000x

Jiahui Hou, [a]‡ Xiaotu Ma, [a]‡ Jinzhao Fu, [a] Panawan Vanaphuti, [a] Zeyi Yao, [a] Yangtao Liu, [a] and Zhenzhen Yang, [b] Yan Wang *[a]

As the economy started to recover from the COVID pandemic, the price of Li2CO3 skyrocketed to the highest. This situation has aggravated concerns on the supply chain for lithium-ion batteries (LIBs). Recycling spent LIBs is a potential solution to alleviate the bottleneck of the supply chain and prevent environmental pollution, which has attracted lots of attention. However, lithium recycling is generally disregarded because of the complex recycling process and its low recycling efficiency. Here, this work developed a sustainable lithium recovery process, which can selectively leach and recover lithium with formic acid before recycling valuable metals. With reported method, lithium can be 99.8% recovered from layered oxide cathode materials with 99.994% purity. In addition, this lithium recovery process is affordable, compared to typical hydrometallurgical process, by saving 11.15% per kilogram spent LIBs. Therefore, this research provided a new settlement on eliminating the effects of lithium ions on valuable metals separation and co-precipitation reaction and precluding the influence of other metal ions on lithium recovery. This simplified lithium recovery process opens up new opportunities for sustainable recycling of LIBs and economical restoration of lithium supply chain.

Introduction

The wide applications of lithium-ion batteries (LIBs) are directly driven by their excellent performance in power sources, mobile electronics, and energy storages.[1-3] Moreover, LIBs dominate the electric vehicle market due to their high energy density, contributing to USD 36.90 billion in 2020 with the increasing demand of electric vehicles (EVs), and will expect to cause approximately 1 million spent LIB packs in 2030.[4-7] However, the increased demands and generated spent LIBs bring concerns to the supply chain and environment. Thus, a sustainable LIBs system must be developed sooner than later.[8]

Lithium is the essential element in LIBs, which is mainly applied in cathode materials and electrolytes. In 2019, 65% of lithium consumption was for battery applications, a 30% increase from 2015, resulting in the most significant source of lithium consumption.[9, 10] From 2018 to 2019, the consumption of lithium rose 18%, from 49,100 tons to 57,700 tons.[10] If the annual growth rate of lithium demand remains 18%, the global lithium reservoir will be inaccessible within 30 years.[10, 11] Meanwhile, due to the long lead time and limit production to mine and brine operations the demand may outstrip supply as early as 2022.[9, 11-13] As the economy recovers from the pandemic, the price of the most common traded forms of battery-grade lithium salt in the global market including Li_2CO_3 and LiOH was increased very significantly in September 2021. The price of battery-grade Li_2CO_3 in 2022 reached $76,700 per ton, which surpasses the previous cost of $24,750 per ton in March 2018. Moreover, LiOH price rose an average of $77.5 per kilogram.[14-17] Whether it is an excessive increase in the price of lithium or an inequality between supply and demand growth of lithium, it will cause a devastating impact to the development of EVs, mobile electronics and energy storages.

As there are 5-7% of lithium in spent LIBs depending on different types of LIBs, recycling is an effective way to reduce the bottleneck of the lithium supply chain and shorten the supply-demand gap of lithium.[18] For example, a single car LIB pack based on $LiNi_{0.5}Mn_{0.3}Co_{0.2}O_2$ contains around 8 kg of lithium.[19] It is predicted that the complete recycling system would reduce the demand for mined lithium to 37%. However, a rare focus was placed on recycling lithium from spent LIBs because it is less expensive than other elements, such as Co. Nevertheless, with the sharp rise in lithium price and the increased number of spent LIBs, the situation starts to be upturned.

The pyrometallurgical recycling process usually extracts target metals via a high-temperature treatment. Although it is simple and easy to scale up, lithium remains challenging to be recovered effectively and always remains in the slag.[20] However, some researchers have investigated further on recycling lithium from the slag via an added hydrometallurgy method. Liu et al.[21] conducted leaching of the roasted products to recycle 93.67% of lithium based on the pyrometallurgical process. Hu et al.[22] reported that 84.7% of lithium was recovered via carbonated water-leaching method in a pyrometallurgical process. Although these methods improve the recycling of lithium, the energy consumption is high.[20] In contrast, the hydrometallurgical recycling process uses aqueous chemical method to decompose target elements into solution. In this process, lithium is usually extracted the last in the solution. Waengwan et al.[23] recycled 75% of lithium at the end of the hydrometallurgy process Solvent extraction. Lv et al.[24] reported a similar work with a recovery rate of 91.23% for lithium. Although the recovery rate is high for both two methods, the extra oxidant and precipitant involved cause the

a. Department of Mechanical and Materials Engineering, Worcester Polytechnic Institute, 100 Institute Rd., Worcester, MA, 01609, USA
b. Chemical Sciences and Engineering Division, Argonne National Laboratory, Lemont, IL 60439, USA

†Electronic Supplementary Information (ESI) available. See DOI: 10.1039/x0xx00000x

‡These authors contribute equally.

extra cost of the recovery process and additional burden for environment. While the hydrometallurgical process has a high recovery rate of lithium, the low concentration of lithium in the raffinate requires an extra concentration process,[20] leading to a high back-end cost. The direct recycling process is a recovery method that directly harvest and recover active materials from LIBs, while retaining their original compound structure.[25, 26] During this process, lithium will not be extracted from spent cathode materials. Extra Li sources will be added to recover the structure and performance of spent cathode materials. Although the recovery rate of lithium seems to reach 100%, strictly sorting, pre-treatment steps and outdated recovered product limit the scale-up of the direct recycling process.[27] In summary, despite the increased interest in lithium recycling, lots of challenges on the commercialization aspects and development of a sustainable process remain.

Here, we developed a highly selective process of lithium extraction via concentrated formic acid leaching. In this process, lithium is preferential extracted with only a trace amount of transition metals (< 5%) leached into the solution. The optimized condition is obtained at 60°C for 5 hours. In addition, all chemicals can be reused via facile distillation process, thereby allowing a fully closed-loop process for environmentally friendly lithium recovery. With the reported method, lithium can be 100% leached from different layered oxides cathode materials where the purity of recovered lithium carbonate can reach as high as 99.994% with 99.8% recovery efficiency, which both reach highest among reported works (**Table S6**).[24, 28-35] Furthermore, lithium can be recovered from leaching solution first, which carries out a new approach to extract Lithium with reusable chemicals to enable a high recycling rate, low expense, and high purity products. Compared to the traditional lithium recycling methods, our approach avoids introducing extra chemicals for lithium extraction. In the hydrometallurgical process, lithium recovery is after co-precipitation reaction from the ammonia solution with a high Na/Li ratio. Our method can eliminate the effects of lithium ions in the co-precipitation reaction and simplify the lithium recovery process and waste water treatment. Besides, the lithium recovery process is cost competitive compared to the hydrometallurgical process, which can save 11.15% cost of recipient per kilogram spent battery.

Experimental

Materials

Formic acid (98%), Acetone (≥ 99.5%), commercial lithium carbonate (Li_2CO_3) used for comparison in this work were purchased from Sigma-Aldrich. $LiNi_{1/3}Mn_{1/3}Co_{1/3}O_2$ (NMC111, MTI), $LiNi_{0.6}Mn_{0.2}Co_{0.2}O_2$ (NMC622, BASF), $LiNi_{0.8}Mn_{0.1}Co_{0.1}O_2$ (NMC811, Targray), black mass (actual spent LIBs powder including mixed cathode materials, graphite, and conductive carbon, commercial recycler) were used in the leaching process. All used materials were dissolved in the acid solution to validate the stoichiometric ratio of the elements by inductively coupled plasma-optical emission spectrometry (ICP-OES). The results are listed in **Table S1**.

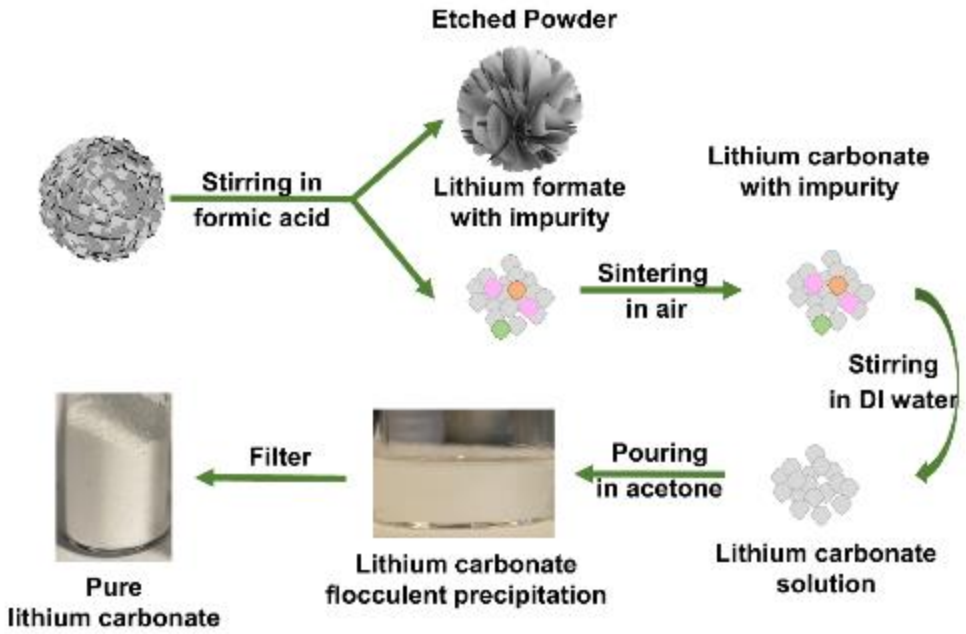

Fig. 1 Simplified schematic of formic acid leaching process, lithium carbonate recovered process and lithium carbonate purified process.

Recycle and Recovery Process

The entire process is illustrated in **Fig. 1.** The selective leaching experiments were conducted in a glass vial while stirring to ensure the good contact area between the cathode materials

and formic acid. During this process, the cathode materials react with formic acid and the products are lithium formate, transition metals formate, oxygen, and water. Taking NMC111 as an example, the reaction formula is displayed in Equation 1.

$$2LiMO_2 + 4HCOOH \rightarrow 2HCOOLi + (HCOO)_2M + 2H_2O + MO_2 \quad (1)$$

The reaction was performed at different temperatures and time to determine the optimized leaching conditions. After leaching, the solid powder was separated from the leaching solution through filtering. Then, the leaching solution was distilled at the set temperature while stirring to recycle the formic acid whereas contaminated Lithium formate was collected for further recovery and purification. The contaminated lithium formate was sintered in the muffle furnace. The whole sintering process was carried out under air atmosphere. The contaminated lithium formate was sintered in the muffle furnace. The whole sintering process was carried out under air. As shown in Equation 2, the lithium formate will react with oxygen producing lithium carbonate, carbon dioxide, and water.[36] The transition metal formate will react with oxygen, producing metal oxide, carbon dioxide, and water (Equation 3-5).[37-40]

$$2HCOOLi + O_2 \rightarrow Li_2CO_3 + CO_2\uparrow + H_2O \quad (2)$$

$$Ni(HCOO)_2 + O_2 \rightarrow NiO + 2CO_2\uparrow + H_2O \quad (3)$$

$$Co(HCOO)_2 + O_2 \rightarrow CoO + 2CO_2\uparrow + H_2O \quad (4)$$

$$Mn(HCOO)_2 + O_2 \rightarrow MnO + 2CO_2\uparrow + H_2O \quad (5)$$

The heating and cooling rates during sintering were maintained at 2°C/min. The sintered powder was dissolved in the deionized water (DI water) at room temperature. After filtering, the lithium carbonate solution was collected. The lithium carbonate was precipitated when transferring the solution into acetone. The recovered lithium carbonate powder was filtered and dried in the regular oven. To purify the used acetone solution, distillation process was performed based on boiling point.

Materials Characterization

All leaching solutions under different conditions, recycled chemicals, and final products were tested by ICP-OES to measure the elements' concentration and calculate the efficiency and purification. Particle crystallinity was examined via X-ray powder diffraction (XRD; PANalytical Empyrean, Cu Kα, λ = 1.54 Å, and scan step size = 0.0167°/step). The morphology and particle size of the materials were observed by a scanning electron microscopy (SEM; JSM 7000F SEM). Recycled formic acid and virgin formic acid were tested by nuclear magnetic resonance (NMR) to determine the molecular structures. Thermogravimetric test of the contaminated lithium formate has been conducted by Simultaneous Thermal Analyzers (SDT Q600-TA Instruments), measuring both heat flow and weight changes of a material as a function of temperature (or time) under controlled atmospheres. X-ray photoelectron spectroscopy (XPS) was conducted by a PHI 500 VersaProbe Ⅱ system from physical electronics to study the oxidation state of metal elements at the particle surface. The XPS fitting spectra were obtained by XPSpeak41 software. The focused ion beam (FIB) and advanced scanning electron microscope (SEM) were conducted by FEI NanoLab 660 DualBeam system for fast cutting and efficient polishing selected particle and scanning images with elements analyzing.

Results and Discussion

Formic acid can be used to selectively leach lithium out from the cathode materials because lithium formate is soluble in the concentrated formic acid whereas the transition metals (TM) formate are insoluble in the concentrated formic acid. [41] To investigate the optimized conditions for formic acid leaching of all layered oxide cathode materials, the effects of reaction time and temperature were thoroughly investigated.

Optimized Conditions of the Leaching Process

Three sets of tests for each leaching conditions were repeated to determine the temperature for the reaction, with the fixed leaching time of 1 hour (As shown in Table S2). $LiNi_{1/3}Mn_{1/3}Co_{1/3}O_2$ (NMC111) was first applied to examine the appropriate temperature condition. As shown in Fig. 2a, the average leaching efficiency of lithium is only 67.28% ± 0.78% at 20°C. Then, the average leaching rate of lithium increases gradually with the increased temperature and reaches 100.01% ± 0.02% at 60°C. However, when the temperature increases to 70°C, the average leaching efficiency decreases to 88.57% ± 0.33% and further decreases to 87.24% ± 0.44% at 80°C. This is due to adhesion of the insoluble salts on particle surfaces that prevent the leaching process. In **Fig. S1**, the shell of TM salts can be seen clearly, and its thickness is increased as temperature increases. Moreover, **Fig. S2** exhibits the morphology of etched NMC111 particles before and after water washing process. Before water washing, the etched powder still has large primary particles and dense secondary particles as shown in **Fig. S2a**. However, after water washing, the large primary particles are unobservable, and the secondary particles show a significant porous structure as shown in **Fig. S2b**. This is because the large primary particles are TMs formate salt particles, which are insoluble in concentrated formic acid.[42] As a result, TMs formate salts will form on the particle surface and prevent the leaching process. Although the leaching rate of TMs has similar trend as lithium, it is under 5% at any given temperature. Therefore, 60°C is the optimized temperature for NMC111 to completely leach lithium out. Subsequently, $LiNi_{0.6}Mn_{0.2}Co_{0.2}O_2$ (NMC622) and $LiNi_{0.8}Mn_{0.1}Co_{0.1}O_2$ (NMC811) were tested at 50°C, 60°C, 70°C and 80°C based on the results of NMC111. As shown in Fig. 2b, the average leaching efficiency of lithium for NMC622 at 50°C, 60°C, 70°C and 80°C is 38.21%±0.48%, 66.47%±0.41, 60.09%±0.78% and 45.28%±0.62 whereas the leaching efficiency of TMs is 1.25%±0.04%, 1.54%±0.05%, 1.11%±0.065 and 1.28%±0.04% respectively. In Fig. 2c, the average lithium leaching efficiency for NMC811 at 50°C, 60°C, 70°C and 80°C is 49.28%±0.46%, 86.70%±1.01%, 81.50%±0.64% and 55.27%±0.57% with average leaching efficiency of TMs is 1.54%±0.03%, 2.99%±0.08%, 2.59%±0.04% and 1.99%±0.04%, respectively. Thus, 60°C is selected as the optimized temperature. The effect of reaction time on leaching efficiency of metals was examined at fixed solid-to-liquid ratio of 20 and

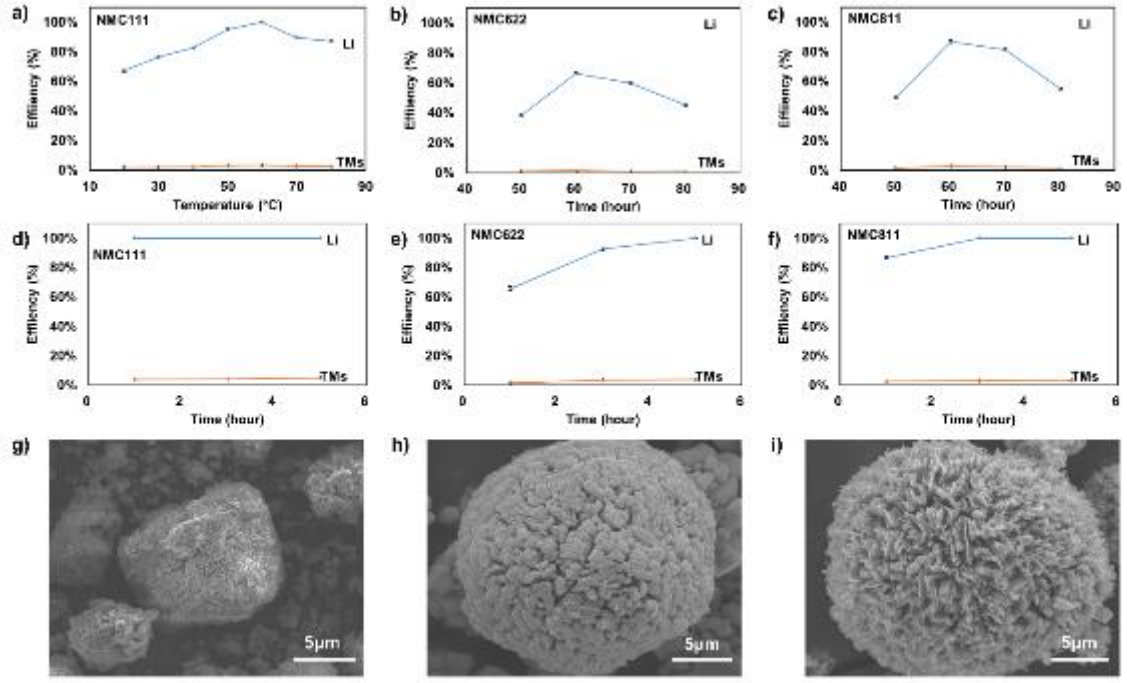

Fig. 2 Li and TMs leaching efficiencies for NMC111, NMC622 and NMC811 at different leaching temperature and time, and SEM images of leached NMC111 at different time and temperature; (a) Li and TMs leaching efficiency for NMC111 at different temperature, (b) Li and TMs leaching efficiency for NMC622 at different temperature, (c) Li and TMs leaching efficiency for NMC811 at different temperature, (d) Li and TMs leaching efficiency for NMC111 at different leaching time, (e) Li and TMs leaching efficiency for NMC622 at different leaching time, (f) Li and TMs leaching efficiency for NMC811 at different leaching time, (g) SEM image of leached NMC111 particles at 80°C for 1 hour, (h) SEM image of leached NMC111 particle at 60°C for 1 hour, and (i) SEM images of leached NMC111 particle at 60°C for 5 hour.

temperature of 60 °C. In **Fig. 2d-f**, the leaching efficiency of all metals keeps increasing as the time extends. In fact, the average leaching efficiency of lithium for NMC111 is 100%±0.01% since the first hour (Fig. 2d), however, the average leaching efficiency of NMC622 and NMC811 is only 65.77%±1.47%, and 86.87%±0.67% after 1 hour, respectively (**Fig. 2e and f**). After 3 hours, the average leaching percentage of lithium for NMC622 is increased to 92.76%±1.22%, and the average leaching percentage of NMC811 increases to 100.01%±0.01%. Furthermore, as the time increases to 5 hours, the average leaching efficiency of lithium increases to 100.01%±0.02% with 3.91%±0.16% of transition metals average leaching efficiency for NMC622, and 3.34%±0.18% for NMC811. As shown in **Fig. 2g**, the NMC111 particles are etched after reacting with the formic acid. As time increases, the particles become more porous as shown in **Fig. 2h-i**, which indicates that both the lithium and TMs are leached out. In short, the optimized leaching conditions are at 60°C for 5 hours where the leaching efficiency of NMC111, NMC622, and NMC811 are all 100% for lithium with less than 5% of TMs.

By considering the reality of recycling manufacturing, the cathode powders are always mixed with different cathode materials, anode powder and carbon black.[43, 44] Thus, to study the effect of mixed powder, two samples including a mixture of NMC111, NMC622 and NMC811, and black mass (actual spent LIBs powder composed of NMC111, $LiMn_2O_4$, graphite anode and conductive carbon) are leached at 60°C for 5 hours and the results have been summarized in **Fig. 3**. Remarkably, the leaching efficiency of lithium for all tested materials can reach 100%, and the average leaching efficiency of TMs for mixed cathode materials and black mass were 4.20%±0.09%, and 5.49%±0.18%, respectively. Especially, the leaching rate of Ni and Co is under 1.5% and the leaching efficiency of Mn is under 3.5%, which considered to be only trace amount.

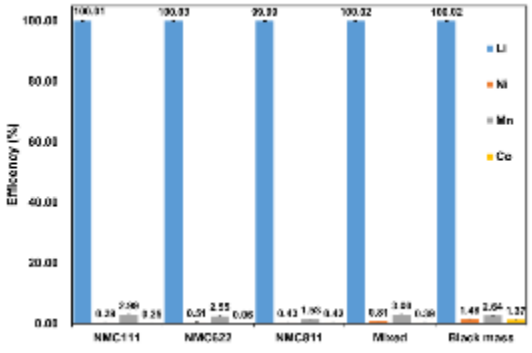

Fig. 3 Selectively leaching performances of the formic acid for NMC111, NMC622, NMC811, mixed materials, and black mass.

Mechanism of leaching process

X-ray photoelectron spectroscopy (XPS) measurements were carried out to investigate the oxidation state of lithium and transition-metals (Ni, Mn, and Co) at the particle surface during the leaching process. The binding energy for C 1s (**Fig. S3**) of Pristine-NMC111(284.87eV), FA-Leached NMC111(284.76eV), and DI-Leached NMC111(284.91eV) was used to do the calibration for all other elements. The peak at ~288eV for

Pristine-NMC111 and DI-Leached NMC111 is usually correlated to O-C=O, which indicated the common impurities on the surface of the carbon tape.[45] However, the ratio of this peak increases to 55.1% for FA-Leached NMC111 particles, which proves that the formate salt is accumulated on the particle surface. As shown in **Fig. 4a-c**, there are two peaks located at 54.07 eV, and 55.1eV in pristine NMC111 cathode materials, which demonstrates that the existence of Li_2O[46] in NMC111 crystal structure and residual Li_2CO_3 on the surface of NMC111. For leached NMC111 particles washed by formic acid (FA-Leached NMC111), the lithium oxide bond (Li-O) can still be detected at 55.0eV, which is contributed by lithium formate.[47] This conclusion can also be confirmed by the ICP results in **Table S3**. The ICP results shows that approximate 0.1% lithium can still be detected in FA-Leached NMC111. Meanwhile, no obvious lithium bond is inspectable by XPS for washed leached NMC111 particles (DI-Leached NMC111) indicating that all lithium ions in NMC have been completely leached out by formic acid and transformed into a water-soluble form. Thus, considering that the metal formate is insoluble in formic acid but highly soluble in water, [48, 49]we assumed that the 0.1% lithium residue is because the lithium formate adhered to the particle surface. The Ni 2p spectrum (**Fig. 4d-f**), presents two spin-orbit lines, of which the Ni 2p 1/2 located at 872.148eV, and Ni 2p 2/3 located at 854.562eV present the existence of Ni^{2+}. The peaks at 873.702eV (2p 1/2), and 855.964eV (2p 2/3) correspond to Ni^{3+} in pristine NMC111. During leaching, NMC111 particles reacted with formic acid producing nickel(Ⅱ) formate, which is insoluble in the concentrated formic acid.[49] As a result of the valence changes during the reaction, in FA-Leached NMC111 (**Fig. 4e**), the peak of Ni^{3+} is slightly shifted to 874.29eV. Meanwhile, the nickel(Ⅱ) formate sticked on the surface of the leached particle and the content of Ni^{2+} increased from 31.52% to 68.56%, calculated by the area of peaks. However, after washed by DI water, the XPS results revealed the decrease of Ni^{2+} attributing to the solubility of Nickel formate in the DI water, therefore, the content of Ni^{2+} dropped back to 32.6%. In **Fig. S3c**, the binding energy of Mn 2p is 641.89eV, 642.7eV, and 641.835eV corresponding to Mn^{3+} cation for Pristine NMC111, FA-Leached NMC111, and DI-Leached NMC111 respectively. The peaks located at 643.66eV, 644.2eV, and 643.46eV for Pristine NMC111, FA-Leached NMC111, and DI-Leached NMC111 respectively, show the existence of Mn^{4+} on the surface of the particle.[50] It is worth to emphasize that on the surface of FA-Leached particle, Mn^{2+} cation is detected, at 641.52eV.[51] This phenomenon further proved that during leaching reaction, manganese(Ⅱ) formate was produced, and then sticked on the surface of the particle. Correspondingly, the manganese (Ⅱ) formate can dissolve into the DI water during the washing process, therefore, Mn^{2+} cannot be detected on the surface of DI-Leached NMC111 particle. The Co 2p spectrum had two main peaks (**Fig. S3b**), 2p 3/2 at 779.8eV and 2p 1/2 at 794.7eV indicating that Co^{3+} is dominant in the crystal structure. The coexistence of Co^{2+} is confirmed with peaks at 781.4eV (2p 3/2), and 796.1eV (2p 1/2). The possible reasons for small peak at 776eV is the O KLL[52], or the peak for cobalt formate.[53] The content of Co^{2+} is 20.9%, 61.65%, and 40.98% in Pristin-NMC111, FA-Leached NMC111, and DI-Leached NMC111, respectively. This result for Co is consistent with results for Ni and Mn, which indicated that the cobalt formate was produced

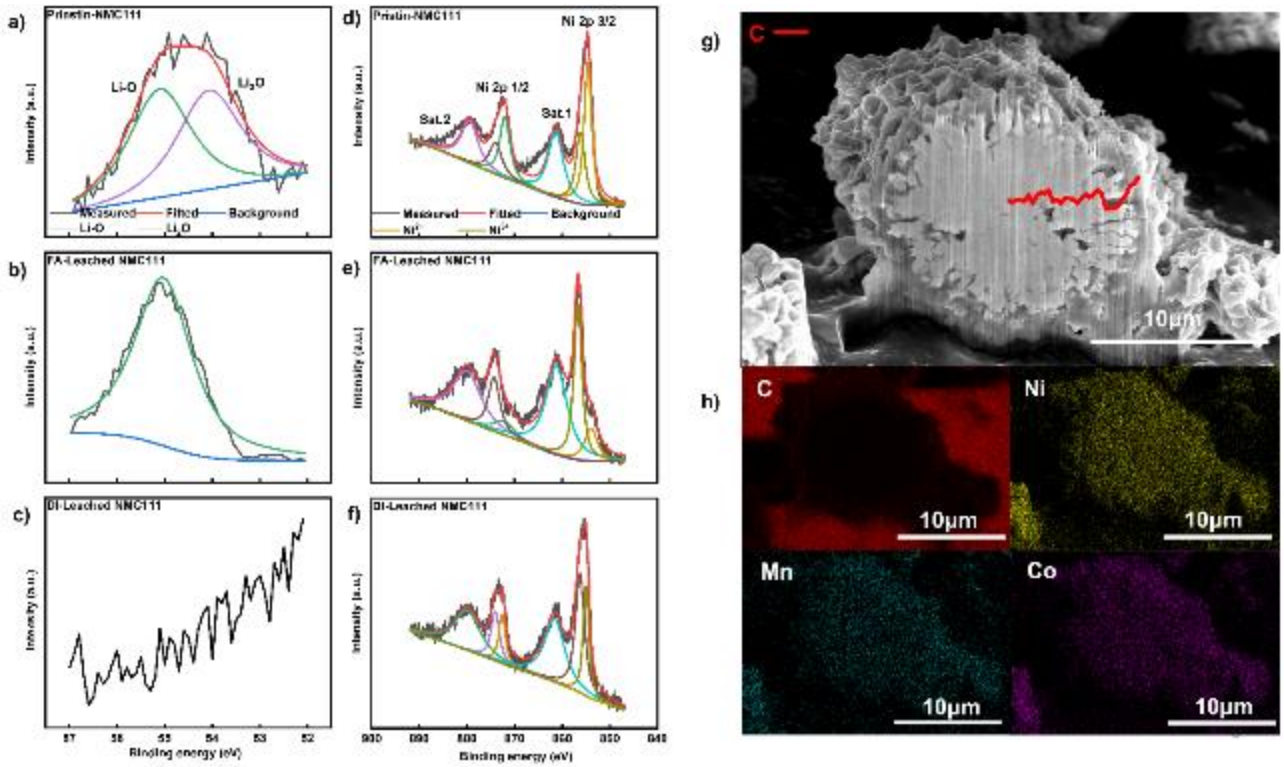

Fig. 4 (a-c) Li 1s valance band for pristine-NMC111, FA-Leached NMC111, and DI-Leached NMC111, (d-f) Ni 2p valance band for pristine-NMC111, FA-Leached NMC111, and DI-Leached NMC111

during leaching reaction and dissolved by DI water during washing.

To further confirm the existence of metal formate adhered on the surface of leached particles, the FA-leached NMC111 was firstly cut by a focus ion beam (FIB) to expose the particle cross-section. Later, the SEM and Energy dispersive spectroscopy (EDS) elements mapping were performed on that cross-section to diagnose the carbon distribution from particle centre to surface. EDS elemental mapping result is shown in **Fig. 4g-h**, and carbon(C), contributing by formate salt, is not detected in the FA-Leached NMC111 particle, however, there is an obvious signal of C at the edge of the particle. The distribution of C presents the existence of formate salt on the surface of the particle. Although the background noise of carbon tape is high, the C signal at the edge of the particle can still be detected. According to the carbon distribution detected, the transition metals were leached out during leaching process, and formed transition metal formate salts. Due to the insolubility of transition metal salts in concentrated formic acid, those formate salts eventually adhered on the surface of the particles. As shown in **Fig. 4h**, the elemental mapping shows a homogeneous distribution of Ni, Mn, and Co in the leached NMC111 particle. Furthermore, the ICP results in **Table S3** show that the ratio of Ni: Mn: Co in FA-Leached NMC111 and DI-Leached NMC111 is approximately 1:1:1, which can also support that the formic acid cannot selectively leach Ni, Mn, and Co from NMC cathode materials.

Lithium recovery

After lithium is leached into the solution with minor formation of TMs formate, the lithium is extracted and purified as Li_2CO_3 by a simple distillation and sintering process. During distillation, the formic acid is evaporated from the flask, and then collected after condensed in the condenser. The formate salts including lithium formate, manganese formate, cobalt formate, and nickel formate are crystallized and collected from the flask. Then, formate salts are decomposed in the sintering process and converted to the mixture of lithium carbonate, manganese oxide, cobalt oxide, and nickel oxide. In order to confirm the transformation, TGA is employed to investigate the decomposition temperature for the mixture of formate salts. In **Fig. 5a**, the weight starts dropping at 30°C due to the dehydration of the formate salts. The second drop occurs at around 230°C, caused by the decomposition from formate to carbonate.[36] The weight kept decreasing till around 350°C where the decomposition of lithium formate is completed. The TMs formate converts to TMs oxide in the range of 230°C to 340°C.[37-40] Therefore, the obtained formate mixture is sintered in a two-step procedure. In the first step, the mixture is sintered at 350°C for 5 hours to convert the lithium formate to lithium carbonate. Then, the temperature is further increased to 450°C in the second step, to ensure all TMs formate is decomposed to insoluble TMs oxide. Therefore, after the sintering process, the lithium carbonate is soluble in the DI water,[54] and the insoluble TMs oxide is filtered out. Then, the lithium carbonate solution is poured into acetone, due to the insolubility of lithium carbonate in acetone[55]. Lithium carbonate forms flocculent

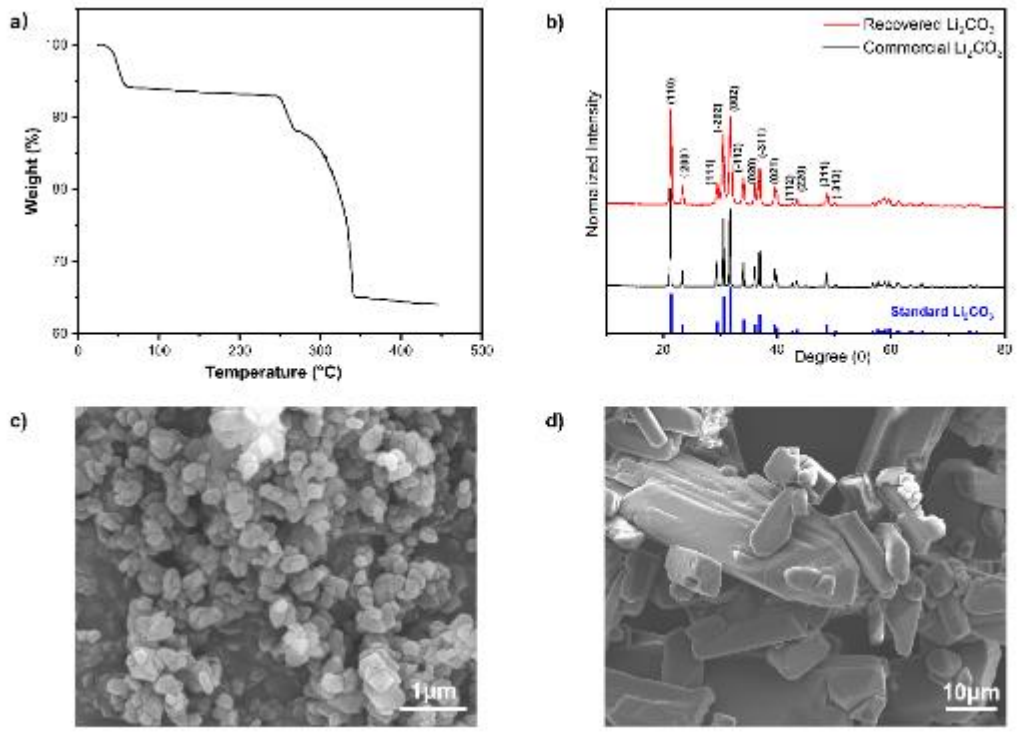

Fig. 5 (a) TGA pattern of contaminated lithium formate, (b) XRD patterns for commercial lithium carbonate and the recovered lithium carbonate, (c) SEM image for the recovered lithium carbonate, and(d) SEM image for commercial lithium carbonate.

precipitation at the bottom of the container. After filtered, the pure lithium carbonate can be obtained. As shown in **Fig. 5b**, the XRD pattern of the recovered lithium carbonate agrees well with the commercial lithium carbonate and no impurity peaks are observed based on standard lithium carbonate pattern (00-022-1141). To compare the morphology of the recovered lithium carbonate and commercial lithium carbonate, SEM is utilized. **Fig. 5c** shows the particle size of the recovered lithium carbonate is ~100 nm and has a significant agglomeration. Compared with the commercial lithium carbonate in **Fig. 5d**, the particle size distribution of the recovered lithium carbonate is more uniform, which may provide better dispersion when mixing with the precursor. Besides, the final recycling rate of lithium reaches 99.8%, which is the highest recycling rate reported so far based on our knowledge.[10] ICP-MS is employed to detect the purity of the recovered lithium carbonate where the commercial lithium carbonate is tested as a reference. Same amounts of the recovered lithium carbonate and commercial lithium carbonate are dissolved in aqua regia solution for ICP-MS testing, and the results are presented in **Table S3**. Compared to the commercial lithium carbonate, the amount of impurity elements in the recovered lithium carbonate is much lower, indicating a higher purity. Based on the equation (6) below, the calculated purity of the recovered lithium carbonate is 99.994%.

$$Purity = \frac{Tested\ weight\ of\ Li_2CO_3}{Actual\ weight\ of\ Li_2CO_3} * 100\% \quad (6)$$

Electrochemical performance of sintered NMC111 with recycled lithium carbonate

For a deeper quality analysis, a batch of $LiNi_{1/3}Mn_{1/3}Co_{1/3}O_2$ (RLi-NMC111) cathode material was synthesized with the recovered lithium carbonate. **Fig. 6a-b** shows the SEM images of Commercial-NMC111, and RLi-NMC111. A typically spherical secondary particle consisting of primary particles was observed. The particle size for Commercial-NMC111 is ~21.59μm, and for RLi-NMC111 is ~ 20.76μm. The phase and structure of Commercial-NMC111, and RLi-NMC111 were analyzed by XRD shown in **Fig. 6c**. The XRD pattern of RLi-NMC111 matched well with Commercial-NMC111, which refers to a typical layered structure. It is worth to emphasize that RLi-NMC111 has higher (003)/ (104) ratio (1.79), while Commercial-NMC111 is 1.63, indicating a lower cation mixing of the RLi-NMC111 cathode material. Therefore, the RLi-NMC111 cathode material is supposed to have a better electrochemical performance. To obtain the lattice data for RLi-NMC111 and Commercial-NMC111, the refinement was used to calculate the structure parameters, which are displayed in **Fig. 6d-e**, and **Table S4**. Compared to Commercial-NMC111 cathode, the RLi-NMC111 manifested the analogous parameters indicated that the RLi-NMC111 sintered by recovered lithium carbonate can reach the comparable performance.

The RLi-NMC111 cathode material is further tested in Li/NMC half-cell and compared with Commercial-NMC111 under the same condition. The electrochemical performance comparison between RLi-NCM111 and Commercial-NMC111 cathode material is illustrated in **Fig. 6f**. In contrast to Commercial-NMC111, the RLi-NMC111 can provide similar initial discharge capacity (152.1 mAh/g vs. 154.7 mAh/g) at 0.1C. For high-rate performances, the comparison between RLi-NMC111 vs. Commercial-NMC111 is 148.3 mAh/g vs. 148.4 mAh/g, 138.9 mAh/g vs. 140.2 mAh/g, 134.1 mAh/g vs. 134.9 mAh/g, 118.4 mAh/g vs. 120.6 mAh/g, and 111.9 mAh/g vs. 111.4 mAh/g, 102.9 mAh/g vs. 104.5 mAh/g, for 0.2C, 0.5C, 1C, 2C, 3C, and 5C respectively. In addition, the cycling test was carried out at 1C

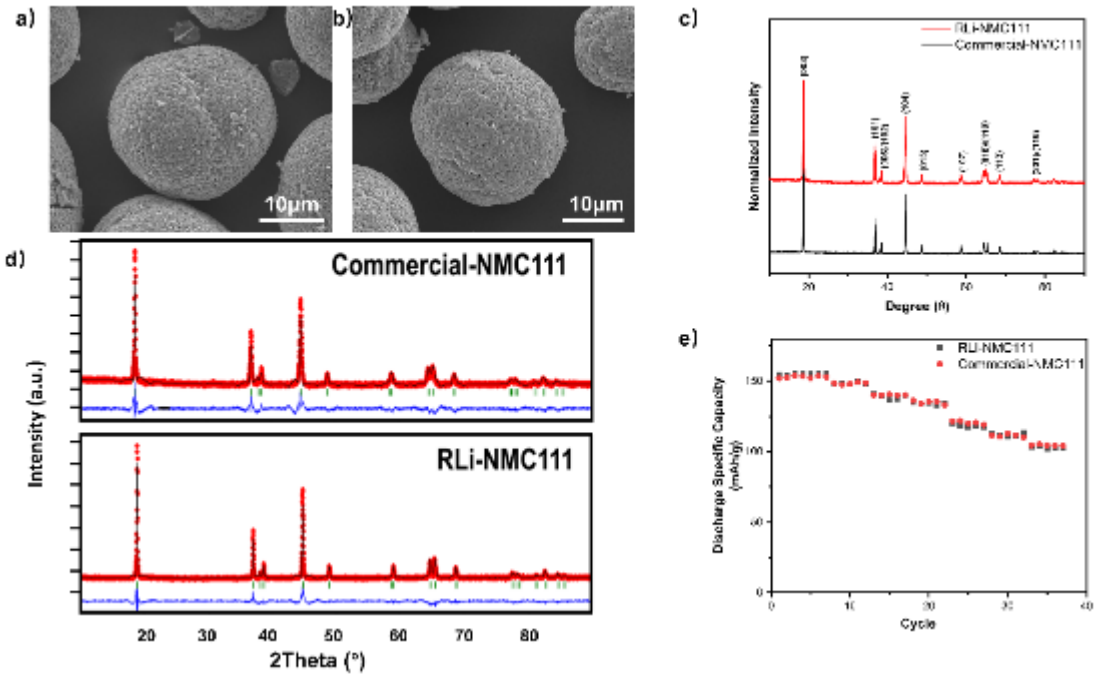

Fig. 6 (a-b) SEM images for Commercial-NMC111, and RLi-NMC111, (b) XRD pattern for Commercial-NMC111, and RLi-NMC111, (c-d) XRD refinement for Commercial- NMC111, and RLi-NMC111, (f) electrochemical performance for TODA NMC111, and RLi-NMC111

with the operating voltage range of 2.8–4.3 V at room temperature. As shown in **Figure S6**, after 50 cycles at 1C, RLi-NMC111 shows comparable cycling stability with Commercial-NMC111.

Above all, the cathode material prepared with recycled Li_2CO_3 is certified to provide matched electrochemical performance compared to Commercial-NMC111 cathode materials.

Development of a closed-loop process

Formic acid has been recycled and collected from the system by a facile distillation process. The density of recycled formic acid is 1.18 g/ml, which is comparable to the virgin formic acid (1.2 g/ml). The decrease in density is due to the close boiling temperature between water produced by the leaching reaction and formic acid. The boiling point of formic acid is 100.8°C, however, the formic acid-water azeotropic mixture has a boiling point at 107°C.[56] Therefore, by introducing water in the recycled formic acid, it is hard to avoid small water contamination during the distillation process. To further confirm the composition of recycled formic acid, NMR is used to determine the different hydrogen bonding in the formic acid and recycled formic acid. **Fig. S4** shows the NMR spectrum for the virgin formic acid and **Fig. S5** shows the NMR spectrum of recycled formic acid. In **Fig. S4**, there are two characteristic peaks for formic acid, the one at 11.03 ppm represents the hydrogen of carboxyl, and the peak at 8.00 ppm refers to the hydrogen for aldehyde.[57] The area for these two peaks is approximately 1:1, which means the amount of two types of hydrogen is similar. Compared to commercial formic acid, the peak for hydrogen of carboxyl shifts to the right due to the presence of water in the recycled formic acid in **Fig. S5.** ICP-MS is tested to further prove the purity of recycled formic acid. As shown in **Table S3**, although the recovered formic acid contains trace metal elements, which is slightly higher than that of commercial formic acid, the recovered formic acid still has high purity. In addition, the recycle efficiency of formic acid is as high as 99.8% where the small inevitable loss is caused by the leaching and distillation processes.

The recycled formic acid can be further utilized in the recycling process. To verify the feasibility, the recycled formic acid is applied in several new recycling processes. The conditions are set at 60°C for 5 hours and the results are summarized in **Fig. 7a**. The average leaching efficiencies of the NMC111, which is leached by the regenerated formic acid, are 100.03%±0.03%, 0.41%±0.04%, 3.44%±0.11% and 0.32%±0.02% for Li, Ni, Mn and Co, respectively. The average leaching efficiency for NMC622 is 100.31%±0.25% of Li with only 0.53%±0.01% of Ni, 3.79%±0.89% of Mn, and 0.66%±0.04% of Co. For NMC811, 100.04%±0.02% of Li can also be leached out, and only 0.46%±0.37%, 3. 70%±0.21%, and 1.09%±0.2% of Ni, Mn and Co, respectively, are leached out with lithium. Same phenomena happen for the average leaching efficiency of black mass, which is 100.01%±0.02% of Li, 2.33%±0.08% of Ni, 3. 47%±0.08% of Mn and 0.32%±0.02% of Co.

In contrast, the leaching efficiency of TMs with the recovered formic acid is slightly higher than that of the virgin formic acid due to the existence of water, which can dissolve more TMs formate salts. However, this is not a concern as TMs formate salts can be converted to insoluble TMs oxide compound during sintering process. Then, it can be collected and combined with insoluble TMs oxide and TMs formate salts in the recycling process.

A green, high efficiency and selective leaching process with formic acid was reported in this work, and the fully closed-loop process is proposed in Fig. 7b. After the leaching process, the lithium-rich solution and the filter cake of TMs formate and TMs oxide can be obtained. Then, the lithium-rich solution undergoes distillation to obtain lithium formate and TMs formate powder. Meanwhile, the formic acid can be recycled by simple distillation method with a recycling efficiency of 99.8%. This can be reused in the recycling scheme. After leaching and purification processes, the TMs products (TMs formate and TMs oxide) are separated from the recovered lithium carbonate and collected for further recycling steps. Lastly, the battery-grade recovered lithium carbonate can be applied in battery material manufacture. Besides, all TMs products can be dissolved in 2.0 M formic acid with H_2O_2 for additional processing. Altogether,

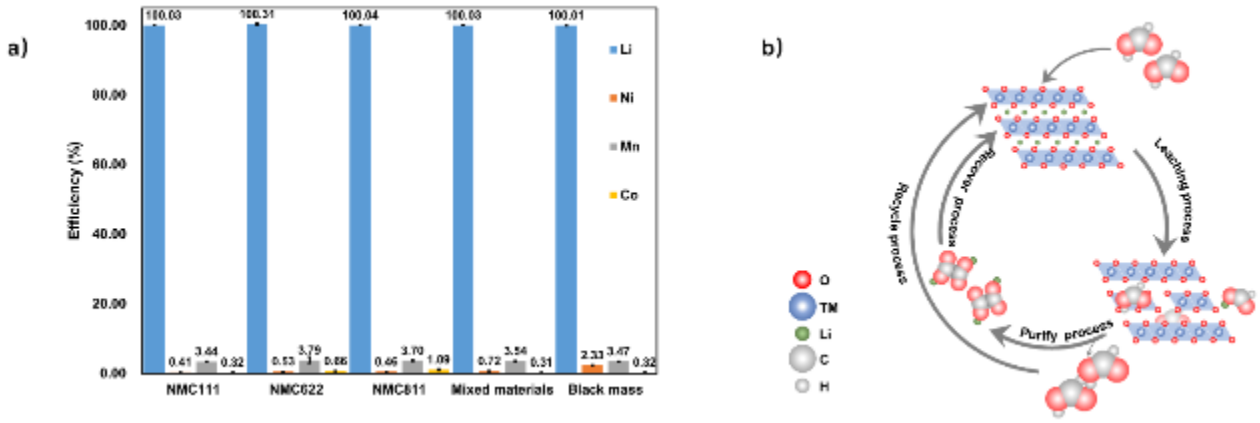

Fig. 7 (a) Selectively leaching performances of the recycled formic acid for NMC111, NMC622, NMC811, mixed materials, and black mass, (b) The closed-loop process for highly selective lithium recovery.

this process does not produce any secondary waste and completely achieve closed-loop recycling of lithium.

Cost analysis

The cost of lithium recovery process is analysed through EverBatt model using the best available information and compared with the results obtained from hydrometallurgical process.[58, 59] The numerical results of this closed-loop lithium recovery process analysis are tabulated in the **Table S5**. The main cost factors and ratio of cost breakdowns contributing to the determination of each recycling process are shown in Figure 8a. For both lithium recovery process and hydrometallurgical process, the most contributing breakdown is direct costs, which are 48.9%, and 46.3% respectively. The direct cost includes equipment, buildings, process and auxiliary, service facilities, yard improvement, and land, which mainly related to the procedure of recycling process. Compared to the default hydrometallurgical recycling process, the closed-loop lithium recovery process does not require the separation of anode and cathode material, and the precipitation of the lithium from the leaching solution. Due to the less equipment involved in, the cost of total capital investment for closed-loop lithium recovery process is 2.03% ($975,148 less) lower than the hydrometallurgical process. The indirect cost contains engineering & supervision fee, and construction expense & contractor fee, which are assumed as 10% of the direct cost in the analysis model. Although the manufacturing cost is only 20.7% and 22.2% of total cost for lithium recovery process and hydrometallurgical process, it contributes a significantly expense reduction by using the closed-loop lithium recovery process, which is 13.37% lower ($3,072,425 less) than the hydrometallurgical process. The direct manufacturing cost demonstrates the cost difference between two recycling process. To further quantify this difference, Figure 8b is created to highlight the cost differences among the main factors. The cost of raw materials account for a great proportion in manufacturing cost, which is 37.58% and 43.02% in lithium recovery process and hydrometallurgical process. The cost difference on raw materials for two recycling process is $1,686,070, which leads to a 54.88% cost gap between lithium recovery process and hydrometallurgical process. For lithium recovery process, although the price of the formic acid, which is the principal chemical used in the closed-loop lithium recovery, is $500-$1000 per tonne,[60] the recyclability of formic acid in the whole process dramatically decreases the cost of raw materials. On contrast, even the major chemicals, such as sulfuric acid, hydrogen peroxide, hydrochloric acid, soda ash, and sodium hydroxide ($66.46, $686.71, $430.22, $150.02, and $400.00 per ton respectively) are all less costly than the formic acid, the expenses on chemicals in hydrometallurgical process are still higher than the lithium recovery process because most chemicals are consumed by the reaction and cannot be recovered. Otherwise, it is worth analysing the differences in waste disposal costs for the lithium recovery and the hydrometallurgical process. The solid waste for hydrometallurgy mainly comes from the current collector and cell shell (Cu, Al, and Fe). In order to deal with these materials $92,700 will be charged every year. During the hydrometallurgical process, 5.8kg (per kg of spent battery recycled) wastewater is generated, which takes $107,174.7 to do the purification to meet emission standards. On contrast, this lithium recovery process can significantly decrease the generation of solid waste and wastewater by eliminating the effect of lithium on metals separation and recycling of used water through the distillation process. Therefore, the cost for dealing with solid waste and wastewater can be dropped to $7,306 and $5,942 per kg of spent battery recycled. Besides, all other expenses are cost of operating labor, supplies, maintenance and repairs, charges of laboratory, and other fixed costs in the EverBatt model. All these terms are calculated based on the fixed capital investment and the findings turn out that they play comparable roles between the two methods. According to the analysis, the total cost to recipient ($/kg spent battery) for lithium recovery process is $2.47, which is lower than the hydrometallurgical process ($2.78). Besides that, this lithium recovery process can directly produce the battery grade

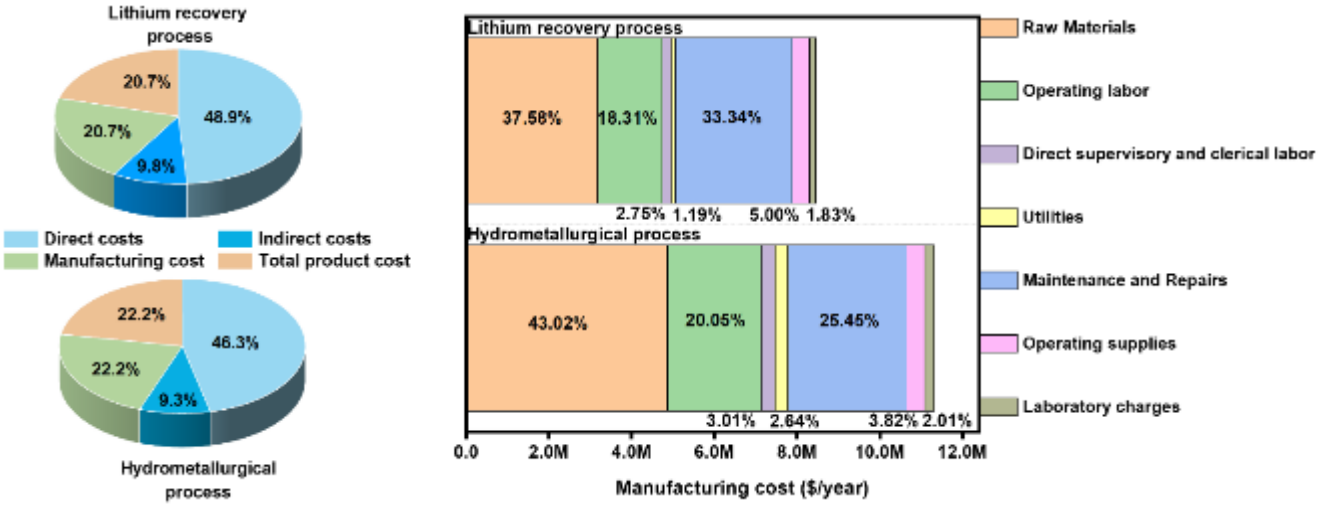

Fig. 8 Cost analysis for hydrometallurgy process and lithium recovery process.

Li_2CO_3 with a recovery rate at 99.8%. However, for default hydrometallurgical process, lithium in the leaching solution is precipitated in the form of Li_2CO_3 by CO_2 or carbonate salt, and the process requires extra concentration and purification process, high temperature treatment, to obtain ~95% purity of Li_2CO_3, which cannot match the requirement for most battery applicatons.[61] For those further concentration, purification process and high temperature treatment, more chemicals, energy, and equipment will be needed, which will significantly increase the cost of recipient. Therefore, the closed-loop lithium recovery process is an affordable method to recovery lithium from spent lithium-ion batteries.

Carbon footprint is essential in evaluating the mitigation potential of climate change and the energy consumption of the recycling process in the life cycle assessment of lithium-ion batteries.[62] Less materials and energy required tend to shift the carbon footprint downward. Compared to the traditional production processes of lithium carbonate, this lithium recovery method avoids the high-temperature treatment. All heat-treatment is lower than 400°C, which can significantly reduce the production of CO_2. In addition, all chemicals used during lithium recovery process can be recycled, which decreased the requirement of the materials. Furthermore, compared to other recycling processes, this lithium recovery process does not produce any wastewater.

Conclusion

In this paper, we develop a highly selective recycling process to recover lithium from spent LIBs with easily degradable formic acid. The selective extraction system exhibited an excellent performance to recover lithium from spent cathode materials. The lithium can be completely extracted with a leaching efficiency of 100% at 60°C for 5 hours in all pure, mixed cathode materials, and black mass from the real recycling process. Other elements are rarely leached out with lithium with leaching efficiency lower than 5%, indicating a highly selective extraction only for lithium. After distillation and sintering processes, the purity of recovered lithium carbonate is as high as 99.994% with an impressive recycling rate of 99.8%. In addition, the formic acid is reusable, which means that our proposed process does not produce any secondary waste. More importantly, this method has been successfully applied to the black mass, which is the real spent materials including different cathode materials, anode materials and conductive carbon. In summary, we developed a new method to selectively recover 99.8% lithium as lithium carbonate with 99.95% purity. In addition, all chemicals and transition metals can be reused via a facile distillation process, thereby allowing a fully closed-loop process for an environmentally friendly lithium recovery process.

Author Contributions

J. Hou, and X. Ma contributed equally.

J. Hou, and X. Ma conceived and designed this work. J. Fu, V. Panawan, Z. Yao, and Y. Liu conducted the investigation, measurements and editing the paper. Z. Yang conducted the XPS measurements. Y. Wang supervised the project.

Conflicts of interest

There is a patent application based on the research results reported in this paper.

Acknowledgements

XPS work was conducted at Post Test Facility of Argonne National Laboratory, operated for DOE Office of Science by UChicago Argonne, LLC, under contract no. DE-AC02-06CH11357.

References

1. Gao, W.; Zhang, X.; Zheng, X.; Lin, X.; Cao, H.; Zhang, Y.; Sun, Z., Lithium Carbonate Recovery from Cathode Scrap of Spent Lithium-Ion Battery: A Closed-Loop Process. *Environmental Science & Technology* **2017,** *51* (3), 1662-1669.

2. Tan, X. F.; McDonald, S. D.; Gu, Q.; Hu, Y.; Wang, L.; Matsumura, S.; Nishimura, T.; Nogita, K., Characterisation of lithium-ion battery anodes fabricated via in-situ Cu6Sn5 growth on a copper current collector. *Journal of Power Sources* **2019,** *415*, 50-61.

3. Ma, X.; Vanaphuti, P.; Fu, J.; Hou, J.; Liu, Y.; Zhang, R.; Bong, S.; Yao, Z.; Yang, Z.; Wang, Y., A universal etching method for synthesizing high-performance single crystal cathode materials. *Nano Energy* **2021,** *87*, 106194.

4. Chen, B.; Ma, X.; Chen, M.; Bullen, D.; Wang, J.; Arsenault, R.; Wang, Y., Systematic Comparison of Al3+ Modified LiNi0.6Mn0.2Co0.2O2 Cathode Material from Recycling Process. *ACS Applied Energy Materials* **2019,** *2* (12), 8818-8825.

5. Ma, X.; Chen, M.; Chen, B.; Meng, Z.; Wang, Y., High-Performance Graphite Recovered from Spent Lithium-Ion Batteries. *ACS Sustainable Chemistry & Engineering* **2019,** *7* (24), 19732-19738.

6. Battery Market Size, Share & Trends Analysis Report by Product (Lead Acid, Li-ion, Nickle Metal Hydride, Ni-cd), by Application (Automotive, Industrial, Portable), by Region, and Segment Forecasts, 2020 - 2027. *Research and markets* **2020**.

7. Lithium-ion Battery Market to Hit USD 193.13 Billion by 2028; Growing Electrification Trend to Augment Growth: Fortune Business Insights™. **2022**.

8. Ma, X.; Chen, M.; Zheng, Z.; Bullen, D.; Wang, J.; Harrison, C.; Gratz, E.; Lin, Y.; Yang, Z.; Zhang, Y.; Wang, F.; Robertson, D.; Son, S.-B.; Bloom, I.; Wen, J.; Ge, M.; Xiao, X.; Lee, W.-K.; Tang, M.; Wang, Q.; Fu, J.; Zhang, Y.; Sousa, B. C.; Arsenault, R.; Karlson, P.; Simon, N.; Wang, Y., Recycled cathode materials enabled superior performance for lithium-ion batteries. *Joule* **2021,** *5* (11), 2955-2970.

9. Tabelin, C. B.; Dallas, J. A.; Casanova, S.; Pelech, T. M.; Bournival, G.; Saydam, S.; Canbulat, I., Towards a low-carbon society: A review of lithium resource availability, challenges and innovations in mining, extraction and recycling, and future perspectives. *Minerals Engineering* **2021,** *163*, 106743.

10. Bae, H.; Kim, Y., Technologies of lithium recycling from waste lithium ion batteries: a review. *Materials Advances* **2021,** *2* (10), 3234-3250.

11. Xu, C.; Dai, Q.; Gaines, L.; Hu, M.; Tukker, A.; Steubing, B., Future material demand for automotive lithium-based batteries. *Communications Materials* **2020,** *1* (1), 99.
12. Harper, G.; Sommerville, R.; Kendrick, E.; Driscoll, L.; Slater, P.; Stolkin, R.; Walton, A.; Christensen, P.; Heidrich, O.; Lambert, S.; Abbott, A.; Ryder, K.; Gaines, L.; Anderson, P., Recycling lithium-ion batteries from electric vehicles. *Nature* **2019,** *575* (7781), 75-86.
13. Cameron Tarry, F. M.-S., Supply Chain for Lithium and Critical Minerals Is … Critical. *CLEARPATH* **2020**.
14. BENCHMARK'S LITHIUM CARBONATE PRICES REACH NEW ALL-TIME HIGHS. **2021**.
15. LITHIUM CARBONATE PRICES BREAK THROUGH $40/KG BARRIER. **2022**.
16. Lithium Prices Have Nearly Doubled In 2022 Amid Insane Commodity Rally. **2022**.
17. The London Metal Exchange has partnered with price reporting agency Fastmarkets to bring greater transparency to pricing for the lithium market. **2022**.
18. Peng, C.; Liu, F.; Aji, A. T.; Wilson, B. P.; Lundström, M., Extraction of Li and Co from industrially produced Li-ion battery waste – Using the reductive power of waste itself. *Waste Management* **2019,** *95*, 604-611.
19. Castelvecchi, D., Electric cars and batteries: how will the world produce enough? *Nature* **2021,** *596*, 336-339.
20. Liu, C.; Lin, J.; Cao, H.; Zhang, Y.; Sun, Z., Recycling of spent lithium-ion batteries in view of lithium recovery: A critical review. *Journal of Cleaner Production* **2019,** *228*, 801-813.
21. Liu, P.; Xiao, L.; Tang, Y.; Chen, Y.; Ye, L.; Zhu, Y., Study on the reduction roasting of spent LiNixCoyMnzO2 lithium-ion battery cathode materials. *Journal of Thermal Analysis and Calorimetry* **2019,** *136* (3), 1323-1332.
22. Hu, J.; Zhang, J.; Li, H.; Chen, Y.; Wang, C., A promising approach for the recovery of high value-added metals from spent lithium-ion batteries. *Journal of Power Sources* **2017,** *351*, 192-199.
23. Waengwan, P.; Eksangsri, T., Recovery of Lithium from Simulated Secondary Resources (LiCO3) through Solvent Extraction. *Sustainability* **2020,** *12* (17).
24. Lv, W.; Wang, Z.; Zheng, X.; Cao, H.; He, M.; Zhang, Y.; Yu, H.; Sun, Z., Selective Recovery of Lithium from Spent Lithium-Ion Batteries by Coupling Advanced Oxidation Processes and Chemical Leaching Processes. *ACS Sustainable Chemistry & Engineering* **2020,** *8* (13), 5165-5174.
25. Shi, Y.; Chen, G.; Liu, F.; Yue, X.; Chen, Z., Resolving the Compositional and Structural Defects of Degraded LiNixCoyMnzO2 Particles to Directly Regenerate High-Performance Lithium-Ion Battery Cathodes. *ACS Energy Letters* **2018,** *3* (7), 1683-1692.
26. Shi, Y.; Chen, G.; Chen, Z., Effective regeneration of LiCoO2 from spent lithium-ion batteries: a direct approach towards high-performance active particles. *Green Chemistry* **2018,** *20* (4), 851-862.
27. Chen, M.; Ma, X.; Chen, B.; Arsenault, R.; Karlson, P.; Simon, N.; Wang, Y., Recycling End-of-Life Electric Vehicle Lithium-Ion Batteries. *Joule* **2019,** *3* (11), 2622-2646.
28. Wang, H.; Huang, K.; Zhang, Y.; Chen, X.; Jin, W.; Zheng, S.; Zhang, Y.; Li, P., Recovery of Lithium, Nickel, and Cobalt from Spent Lithium-Ion Battery Powders by Selective Ammonia Leaching and an Adsorption Separation System. *ACS Sustainable Chemistry & Engineering* **2017,** *5* (12), 11489-11495.
29. Chen, W.-S.; Ho, H.-J., Recovery of Valuable Metals from Lithium-Ion Batteries NMC Cathode Waste Materials by Hydrometallurgical Methods. *Metals* **2018,** *8* (5).
30. Atia, T. A.; Elia, G.; Hahn, R.; Altimari, P.; Pagnanelli, F., Closed-loop hydrometallurgical treatment of end-of-life lithium ion batteries: Towards zero-waste process and metal recycling in advanced batteries. *Journal of Energy Chemistry* **2019,** *35*, 220-227.
31. Li, Q.; Fung, K. Y.; Xu, L.; Wibowo, C.; Ng, K. M., Process Synthesis: Selective Recovery of Lithium from Lithium-Ion Battery Cathode Materials. *Industrial & Engineering Chemistry Research* **2019,** *58* (8), 3118-3130.
32. Peng, C.; Liu, F.; Wang, Z.; Wilson, B. P.; Lundström, M., Selective extraction of lithium (Li) and preparation of battery grade lithium carbonate (Li2CO3) from spent Li-ion batteries in nitrate system. *Journal of Power Sources* **2019,** *415*, 179-188.
33. Maroufi, S.; Assefi, M.; Khayyam Nekouei, R.; Sahajwalla, V., Recovery of lithium and cobalt from waste lithium-ion batteries through a selective isolation-suspension approach. *Sustainable Materials and Technologies* **2020,** *23*, e00139.
34. Xu, L.; Chen, C.; Fu, M.-L., Separation of cobalt and lithium from spent lithium-ion battery leach liquors by ionic liquid extraction using Cyphos IL-101. *Hydrometallurgy* **2020,** *197*, 105439.
35. Zhang, Y.; Wang, W.; Hu, J.; Zhang, T.; Xu, S., Stepwise Recovery of Valuable Metals from Spent Lithium Ion Batteries by Controllable Reduction and Selective Leaching and Precipitation. *ACS Sustainable Chemistry & Engineering* **2020,** *8* (41), 15496-15506.
36. Meisel, T.; Halmos, Z.; Seybold, K.; Pungor, E., The thermal decomposition of alkali metal formates. *Journal of Thermal Analysis and Calorimetry* **1975,** *7* (1), 73-80.
37. Galwey, A. K.; Brown, M. E., A Differential Scanning Calorimetric Study of the Thermal Decomposition of Nickel Formate Dihydrate. *Proceedings of the Royal Irish Academy. Section B: Biological, Geological, and Chemical Science* **1977,** *77*, 465-471.
38. Arii, T.; Kishi, A., Thermal dehydration of cobalt and zinc formate dihydrates by controlled-rate thermogravimetry (CRTG) and simultaneous X-ray diffractometry–differential scanning calorimetry (XRD-DSC). *Thermochimica Acta* **1999,** *325* (2), 157-165.
39. Rao, G. R.; Patil, K. C.; Rao, C. N. R., Spectra and thermal decompositions of metal formates. *Inorganica Chimica Acta* **1970,** *4*, 215-218.
40. Gómez-Aguirre, L. C.; Otero-Canabal, J.; Sánchez-Andújar, M.; Señarís-Rodríguez, M. A.; Castro-García, S.; Pato-Doldán, B., Thermal Decomposition of [AH][M(HCOO)3] Perovskite-Like Formates. *Solids* **2021,** *2* (2).
41. Hietala, J.; Vuori, A.; Johnsson, P.; Pollari, I.; Reutemann, W.; Kieczka, H., Formic Acid. In *Ullmann's Encyclopedia of Industrial Chemistry*, pp 1-22.
42. Kendall, J.; Adler, H., COMPOUND FORMATION AND SOLUBILITY IN SYSTEMS OF THE TYPE, FORMIC ACID:METAL FORMATE. *Journal of the American Chemical Society* **1921,** *43* (7), 1470-1481.
43. Ma, X.; Azhari, L.; Wang, Y., Li-ion battery recycling challenges. *Chem* **2021,** *7* (11), 2843-2847.
44. Liu, Y.; Zhang, R.; Wang, J.; Wang, Y., Current and future lithium-ion battery manufacturing. *iScience* **2021,** *24* (4), 102332.
45. Pişkin, B.; Savaş Uygur, C.; Aydınol, M. K., Mo doping of layered Li (NixMnyCo1-x-y-zMz)O2 cathode materials for lithium-ion batteries. *International Journal of Energy Research* **2018,** *42* (12), 3888-3898.
46. Aurbach, D.; Pollak, E.; Elazari, R.; Salitra, G.; Kelley, C. S.; Affinito, J., On the Surface Chemical Aspects of Very High Energy Density, Rechargeable Li–Sulfur Batteries. *Journal of The Electrochemical Society* **2009,** *156* (8), A694.
47. Schwenke, K. U.; Solchenbach, S.; Demeaux, J.; Lucht, B. L.; Gasteiger, H. A., The Impact of CO2 Evolved from VC and FEC during Formation of Graphite Anodes in Lithium-Ion Batteries. *Journal of The Electrochemical Society* **2019,** *166* (10), A2035-A2047.

48. Sue, K.; Suzuki, A.; Suzuki, M.; Arai, K.; Hakuta, Y.; Hayashi, H.; Hiaki, T., One-Pot Synthesis of Nickel Particles in Supercritical Water. *Industrial & Engineering Chemistry Research* **2006,** *45* (2), 623-626.
49. Kendall, J.; Adler, H., COMPOUND FORMATION AND SOLUBILITY IN SYSTEMS OF THE TYPE, FORMIC ACID: METAL FORMATE. *Journal of the American Chemical Society* **1921,** *43* (7), 1470-1481.
50. Chen, Z.; Wang, J.; Chao, D.; Baikie, T.; Bai, L.; Chen, S.; Zhao, Y.; Sum, T. C.; Lin, J.; Shen, Z., Hierarchical Porous LiNi1/3Co1/3Mn1/3O2 Nano-/Micro Spherical Cathode Material: Minimized Cation Mixing and Improved Li+ Mobility for Enhanced Electrochemical Performance. *Scientific Reports* **2016,** *6* (1), 25771.
51. Miao, R.; He, J.; Sahoo, S.; Luo, Z.; Zhong, W.; Chen, S.-Y.; Guild, C.; Jafari, T.; Dutta, B.; Cetegen, S. A.; Wang, M.; Alpay, S. P.; Suib, S. L., Reduced Graphene Oxide Supported Nickel–Manganese–Cobalt Spinel Ternary Oxide Nanocomposites and Their Chemically Converted Sulfide Nanocomposites as Efficient Electrocatalysts for Alkaline Water Splitting. *ACS Catalysis* **2017,** *7* (1), 819-832.
52. Millican, S. L.; Androshchuk, I.; Tran, J. T.; Trottier, R. M.; Bayon, A.; Al Salik, Y.; Idriss, H.; Musgrave, C. B.; Weimer, A. W., Oxidation kinetics of hercynite spinels for solar thermochemical fuel production. *Chemical Engineering Journal* **2020,** *401*, 126015.
53. Lermontov, A. S.; Girardon, J.-S.; Griboval-Constant, A.; Pietrzyk, S.; Khodakov, A. Y., Chemisorption of C3 hydrocarbons on cobalt silica supported Fischer–Tropsch catalysts. *Catalysis Letters* **2005,** *101* (1), 117-126.
54. Miller, R. R.; Smith, S. H.; Williams, D. D., Solubility of lithium carbonate at elevated temperatures. *Journal of Chemical & Engineering Data* **1971,** *16* (1), 74-75.
55. РАБИНОВИЧ В.А., Х. З. Я. К. Х. С. И., П Е Р Е Р .И ДОП., *Краткий химический справочник. Изд.2, перер.и доп.* 2012.
56. García-Payo, M. C.; Rivier, C. A.; Marison, I. W.; von Stockar, U., Separation of binary mixtures by thermostatic sweeping gas membrane distillation: II. Experimental results with aqueous formic acid solutions. *Journal of Membrane Science* **2002,** *198* (2), 197-210.
57. Griesbaum, K.; Zwick, G., Diozonolysen von acyclischen konjugierten Dienen in Methanol. *Chemische Berichte* **1986,** *119* (1), 229-243.
58. Lander, L.; Cleaver, T.; Rajaeifar, M. A.; Nguyen-Tien, V.; Elliott, R. J. R.; Heidrich, O.; Kendrick, E.; Edge, J. S.; Offer, G., Financial viability of electric vehicle lithium-ion battery recycling. *iScience* **2021,** *24* (7), 102787.
59. Dai, Q.; Spangenberger, J. S.; Ahmed, S.; Gaines, L.; Kelly, J. C.; Wang, M. Q. In *EverBatt: A Closed-loop Battery Recycling Cost and Environmental Impacts Model*, 2019.
60. Made-in-China product directory. https://www.made-in-china.com/productdirectory.do?word=formic+acid&file=&searchType=0&subaction=hunt&style=b&mode=and&code=0&comProvince=nolimit&order=0&isOpenCorrection=1&org=top.
61. Yao, Y.; Zhu, M.; Zhao, Z.; Tong, B.; Fan, Y.; Hua, Z., Hydrometallurgical Processes for Recycling Spent Lithium-Ion Batteries: A Critical Review. *ACS Sustainable Chemistry & Engineering* **2018,** *6* (11), 13611-13627.
62. Tao, Y.; Rahn Christopher, D.; Archer Lynden, A.; You, F., Second life and recycling: Energy and environmental sustainability perspectives for high-performance lithium-ion batteries. *Science Advances 7* (45), eabi7633.